INFECTION AND IMMUNITY, Jan. 2009, p. 23–31 Vol. 77, No. 1
0019-9567/09/$08.00+0 doi:10.1128/IAI.00801-08

The Mechanism of *Bacillus anthracis* Intracellular Germination Requires Multiple and Highly Diverse Genetic Loci[▽]

Soumitra Barua,[1] Matthew McKevitt,[1] Kevin DeGiusti,[1] Elaine E. Hamm,[1] Jason Larabee,[1] Salika Shakir,[1] Katie Bryant,[1] Theresa M. Koehler,[2] Steven R. Blanke,[3] David Dyer,[1] Allison Gillaspy,[1] and Jimmy D. Ballard[1]*

Department of Microbiology and Immunology, The University of Oklahoma Health Sciences Center, Oklahoma City, Oklahoma 73104[1]; Department of Microbiology and Molecular Genetics, The University of Texas-Houston Health Sciences Center Medical School, Houston, Texas 77030[2]; and Department of Microbiology and the Institute for Genomic Biology, University of Illinois, Urbana, Illinois 68101[3]

Received 27 June 2008/Returned for modification 13 August 2008/Accepted 9 October 2008

In an effort to better understand the mechanisms by which *Bacillus anthracis* establishes disease, experiments were undertaken to identify the genes essential for intracellular germination. Eighteen diverse genetic loci were identified via an enrichment protocol using a transposon-mutated library of *B. anthracis* spores, which was screened for mutants delayed in intracellular germination. Fourteen transposon mutants were identified in genes not previously associated with *B. anthracis* germination and included disruption of factors involved in membrane transport, transcriptional regulation, and intracellular signaling. Four mutants contained transposon insertions in *gerHA*, *gerHB*, *gerHC*, and *pagA*, respectively, each of which has been previously associated with germination or survival of *B. anthracis* within macrophages. Strain MIGD101 (named for macrophage intracellular germination defective 101) was of particular interest, since this mutant contained a transposon insertion in an intergenic region between BAs2807 and BAs2808, and was the most highly represented mutant in the enrichment. Analysis of *B. anthracis* MIGD101 by confocal microscopy and differential heat sensitivity following macrophage infection revealed ungerminated spores within the cell. Moreover, *B. anthracis* MIGD101 was attenuated in cell killing relative to the parent strain. Further experimental analysis found that *B. anthracis* MIGD101 was defective in five known *B. anthracis* germination pathways, supporting a mechanism wherein the intergenic region between BAs2807 and BAs2808 has a global affect on germination of this pathogen. Collectively, these findings provide insight into the mechanisms supporting *B. anthracis* germination within host cells.

Bacillus anthracis spores germinate during early stages of inhalational anthrax, and this is considered to be a critical step in the progression of anthrax disease (4, 5, 7). Indeed, transition from dormant spore to vegetative bacilli is essential for growth, bacteremia, toxin production, and synthesis of a poly-D-glutamic acid capsule, each of which is important to the virulence of *B. anthracis*.

Results from a series of studies indicate *B. anthracis* spores are engaged by, and can germinate within, alveolar macrophages (13, 15). Sanz et al. recently described the detection of *B. anthracis* spores in alveolar macrophages under in vivo infection conditions using a mouse model of inhalational anthrax (15). The molecular basis of spore tropism for alveolar macrophages may be due to the collagenlike exosporium protein, BclA, which interacts with the macrophage receptor, Mac-1 (13), while at the same time preventing the interaction of spores with other types of cells. Spores are taken up by Mac-1-dependent phagocytosis into LAMP-1 positive vesicles, where germination is triggered, and the germinated spores become susceptible to killing by the macrophage (10).

Very little is known about the bacterial factors that promote, repress, or otherwise regulate germination of *B. anthracis* spores within macrophages. To date, experiments have focused on genes predicted to be involved in germination based on homology with genes from other well-studied *Bacillus* species. Guidi-Rontani et al. found that genes in the *gerX* operon support germination of *B. anthracis* in macrophages and in vivo (8). A report from Weiner and Hanna indicates the *gerH* operon is necessary for efficient germination of *B. anthracis* spores engulfed by macrophages (16). Deletion of the *gerS* gene has also been found to attenuate germination within macrophages (11). These findings indicate the *gerH* and *gerX* operons and the *gerS* gene contribute to the germination of *B. anthracis* spores within phagocytic cells.

Homologs of *gerH* operon, *gerX* operon, and the *gerS* genes are also found in nonpathogenic *Bacillus* species (8, 11). However, previous studies by Ireland and Hanna found that nonpathogenic *Bacillus* species do not germinate and survive in macrophages (11). This observation suggests *B. anthracis* may encode yet-unidentified factors necessary for this pathogen's mechanism of intracellular germination. In order to gain insight into these mechanisms of intracellular germination, we developed an experimental approach to screen the genome of *B. anthracis* Sterne 7702 for genes essential for germination within cultured macrophages. The results from the present study support a model in which intracellular germination of *B.*

* Corresponding author. Mailing address: University of Oklahoma Health Sciences Center, BRC-362A, 975 NE 10th St., Oklahoma City, OK 73104. Phone: (405) 271-3855. Fax: (405) 271-3874. E-mail: jimmy-ballard@ouhsc.edu.
▽ Published ahead of print on 20 October 2008.

anthracis spores requires highly diverse genes, which collectively contribute to this critical step in the establishment of disease.

MATERIALS AND METHODS

Bacterial strains, plasmids, cell lines, and chemical reagents. Bacterial cultures of *B. anthracis* or *Escherichia coli* were grown at 37°C in Luria-Bertani (LB) or brain heart infusion medium (Becton Dickinson, Sparks, MD) containing antibiotics at the following concentrations when appropriate: ampicillin, 100 μg/ml; chloramphenicol, 20 μg/ml; kanamycin, 25 μg/ml (for *E. coli*); erythromycin, 5 μg/ml; kanamycin, 100 μg/ml (for *B. anthracis*); and gentamicin, 10 μg/ml. The experiments described here were performed using the Sterne 7702 strain ($pXO1^+$ $pXO2^-$) of *B. anthracis* (2) as the background strain for constructing mini-*Himar1*-Km^r transposon library. Construction and characterization of the mini-*Himar1*-Km^r cassette and generation of the mutant library will be described elsewhere (S. M. McGillivray et al., unpublished data). Construction of a Δ*gerHA* strain of *B. anthracis* has been previously described by McKevitt et al. (12). Abelson murine leukemia virus-transformed murine macrophages derived from ascites of BALB/c mice (termed RAW 264.7) were obtained from the American Type Culture Collection (Manassas, VA). The RAW 264.7 cell line was maintained in tissue culture-grade T-75 flasks grown in the presence of Dulbecco modified essential medium (DMEM; Gibco) supplemented with 10% fetal bovine serum (FBS; American Type Culture Collection) at 37°C with 5.0% CO_2 in a humidified incubator. In all experiments, RAW 264.7 cells were passed fewer than 10 times prior to infection.

Spore preparation. Spores of the *B. anthracis* Sterne 7702 parent strain and the *B. anthracis* mini-*Himar1* transposon library were generated in sporulation medium containing 0.6 mM $CaCl_2 \cdot 2H_2O$, 0.8 mM $MgSO_4 \cdot 7H_2O$, 0.3 mM $MnSO_4 \cdot H_2O$, 85.5 mM NaCl, and 8 g of nutrient broth/liter (pH 6.0). After 3 days of incubation at 30°C, spores were harvested by centrifugation at 7,000 rpm for 15 min at 4°C. After the supernatant was removed, the spore pellet was resuspended in 10 ml of sterile double-distilled H_2O (ddH_2O) and cultured at 30°C for two more days with constant shaking to promote further sporulation and bacterial lysis. Complete spore development was monitored by phase-contrast microscopy. The spore suspensions were finally passed through two inline glass microfiber syringe filters (3.1- and 1.2-μm pore sizes, respectively; VWR) to remove vegetative cells from the spore suspension. Finally, these spores were centrifuged at 7,000 rpm for 15 min at 4°C, washed five times with sterile ddH_2O, resuspended in 1 ml of sterile ddH_2O, and stored at −20°C. Before use, all spore suspensions were diluted to the working concentrations necessary for the corresponding experiments and heated to 70°C for 45 min to kill any residual vegetative cells and germinated or germinating spores, as well as to heat activate the spores. Serial dilutions of the spore preparation were plated on brain heart infusion agar plates to determine the concentration of the CFU prior to experimental analysis.

Enrichment of *B. anthracis* mini-*Himar1* transposon mutants delayed in germination. Approximately 1.5×10^6 murine macrophage RAW 264.7 cells were cultured in six-well tissue culture plates (Becton Dickinson) in a total of 2 ml of DMEM with 10% FBS. Cells were allowed to grow overnight at 37°C in 5.0% CO_2 atmosphere, resulting in a semiconfluent monolayer of cells. After the overnight culture medium was removed, the cells were washed once with 2 ml of DMEM–10% FBS. Macrophages were then infected with *B. anthracis* Sterne mini-*Himar1* transposon library spores at a multiplicity of infection (MOI) of 10 in 2 ml of DMEM–10% FBS. To increase the close contact of spores with macrophages, the plates were centrifuged at $250 \times g$ for 10 min, and 1.5 ml of medium supernatant was removed, leaving 500 μl covering the tissue culture cell layer. After a 90-min incubation of cells and spores at 37°C in a 5.0% CO_2 atmosphere at an MOI of 10, the macrophages were washed 10 times with culture medium to remove the remaining extracellular nonengulfed spores and germinated vegetative cells. Next, the macrophages were incubated in DMEM–10% FBS supplemented with 10 μg of gentamicin/ml for 30 min to kill any remaining vegetative bacilli. The cells were then washed three to five times with phosphate-buffered saline (PBS), after which 500 μl of sterile ddH_2O was added to each well. The cells were scraped off the well surface, passed through a 1-ml pipette 7 to 10 times, and incubated 45 min at 70°C. Finally, the whole volume of 500 μl was inoculated into 5 ml of rich medium and grown overnight. Fresh spores were prepared from the culture and used to infect macrophages. In total, this process was repeated four times to enrich for mutants exhibiting delayed germination under these conditions.

RATE analysis of mini-*Himar1* insertion sites. To determine the mini-transposon insertion site, we took advantage of the rapid-amplification-of-transposon-ends (RATE) reaction (14). Genomic DNA was isolated from 136 randomly picked single colony isolates from the final enrichment step of the *B. anthracis* Sterne 7702 transposon library by using a DNeasy Blood & Tissue kit (Qiagen). Kan-RATE1 primer 5′-CCCTACACAAATTGGGAGATA-3′ was used for the first PCR, and Kan-SEQ1 primer 5′-AATCTAGCGAGGGCTTTACTA-3′ was used for sequencing PCR. In the first step, inward Kan-RATE1 primer (1 μl of 100 ng/μl) was used for the PCR with ca. 200 to 300 ng of the respective mutant genomic DNA as a template. The thermocycler conditions were as follows. After an initial denaturation for 60 s at 94°C, 20 cycles of 94°C for 30 s, 55°C for 30 s, and 72°C for 3 min were performed. This was followed by another 30 cycles of 94°C for 30 s, 30°C for 30 s, and 72°C for 3 min and 30 cycles of 94°C for 30 s, 55°C for 30 s, and 72°C for 2 min, with a final 10 min of extension at 72°C.

Shrimp alkaline phosphatase (SAP) and exonuclease I treatment was carried out on the PCR product pool to dephosphorylate and degrade any residual primer and allow direct sequencing with the specific outward sequencing primer Kan-SEQ1 primer 5′-AATCTAGCGAGGGCTTTACTA-3′. To accomplish this, 8 μl of PCR product was transferred to a new tube and subjected to the following treatment. A master mix of SAP/exonuclease I was prepared as by using 0.05 μl of exonuclease I (Epicenter), 0.5 μl of SAP (Roche), 0.5 μl of SAP 10× buffer, and 10.3 μl of sequencing-grade (deionized ultrafiltrate or 18 Ω) water with a total volume of 11.35 μl. Finally, 10 μl of the master mix described above was added to 8 μl of RATE PCR product, followed by incubation at 37°C for 60 min and 85°C for 15 min and then sequencing.

To determine the sites of transposon insertion, a kanamycin sequence was trimmed from the 5′ ends and low-quality data was trimmed from the 3′ end, and these sequences were subjected to a BLASTn analysis, making direct comparisons with the reported sequence of the *B. anthracis* Sterne strain. In all cases, only significant hits (e value cutoff of $<10^{-4}$) are listed.

Macrophage viability and cytotoxicity assays by trypan blue staining and LDH release following spore infection. RAW 264.7 cells were analyzed for viability after spore infection using trypan blue staining and cytotoxicity was measured as cell membrane lysis and the release of lactate dehydrogenase (LDH) into the culture medium. Samples of culture media from wells containing infected cells were collected at sequential time points postinfection. Levels of LDH were assayed by using the colorimetric CytoTox 96 assay kit (Promega) according to the instructions of the manufacturers. After a 30-min incubation with the substrate mix, the reaction was stopped, and absorbance at 490 nm was determined with an automatic microtiter plate reader (Molecular Devices Corp., Sunnyvale, CA). Total LDH release was achieved by adding Triton X-100 (100 μl/well of a 9% solution) to untreated macrophages. The percentage of LDH release was calculated by dividing the amount of LDH released from infected cells (i.e., experimental − bacterial spontaneous − macrophage spontaneous) by the amount of total LDH (i.e., total macrophage − macrophage spontaneous) and multiplying that value by 100.

At the indicated time points, cells were harvested and, after a 3-min incubation with trypan blue, pictures were taken by using an IX51 Olympus microscope with a DP70 camera.

Visualization and tracking of labeled spores by confocal microscopy. To assess the ability of spores to survive and germinate inside the murine macrophage, spore internalization and spore germination were qualitatively determined by confocal microscopy. Spores were labeled with an Alexa Fluor 488 protein labeling kit (Molecular Probes) for detection by confocal fluorescence microscopy. First, 10^{10} spores were diluted into 10 ml of ddH_2O (Sigma Aldrich) containing 50 mM sodium bicarbonate (pH ~8.3) and gently mixed well. Alexa Fluor 488 dye was added to 750 μl of this spore solution, followed by mixing. The labeled spore solution was then allowed to react with the remaining spores for 1 h at room temperature with gentle agitation according to the manufacturer's protocol for labeling proteins. Unconjugated dye was removed from the labeling reaction by performing five washes with nanopure H_2O. After the final wash, the spores were resuspended in nanopure H_2O (~ 10^9 spores/μl) and stored at −20°C prior to experimentation. Spore viability was not decreased by the fluorophore, as confirmed by plate counts.

RAW 264.7 cells were seeded onto 12-well plates with glass coverslips at a density of 1.5×10^5 cells/well in a final volume of 1 ml and allowed to adhere overnight. The following day, macrophages were infected with Alexa Fluor 488-labeled spores at an MOI of 1 in 1 ml of DMEM–10% FBS, centrifuged at $250 \times g$ for 10 min to enhance adhesion, and incubated for 30 min to facilitate uptake. Next, 10 μg of gentamicin/ml was added, and the macrophages were further incubated for 30 min to kill the extracellular vegetative form. After three to five rinses with fresh DMEM–10% FBS, the cells were allowed to incubate for 1, 6, and 12 h at 37°C in 5% CO_2. Macrophages were then washed three to five times with PBS to remove extracellular spores and vegetative organisms and fixed in freshly prepared 4% paraformaldehyde for 15 min at room temperature.

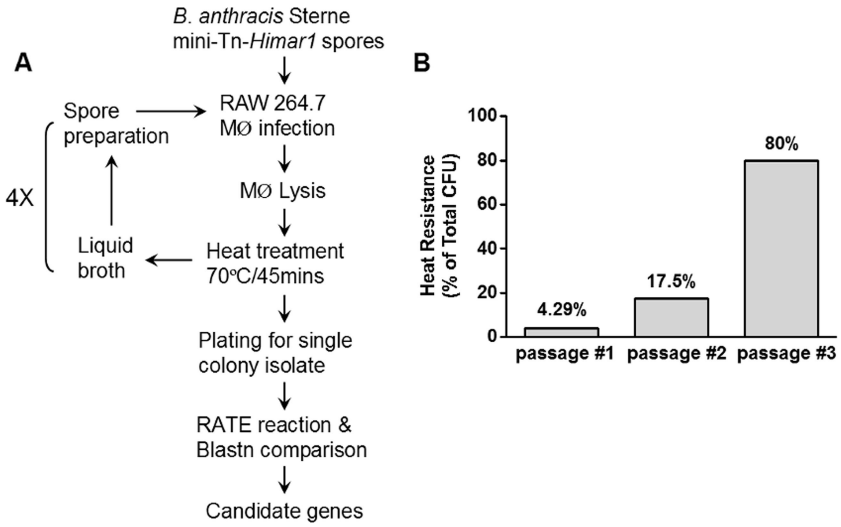

FIG. 1. Enrichment protocol used to identify genes important for *B. anthracis* germination within cultured macrophages. (A) Flowchart outlining the critical steps in the enrichment protocol. The specific details are described in Materials and Methods. Briefly, spores were prepared from a *B. anthracis* Sterne 7702 Himar1 library, and these were used to infect cultured macrophages (Mϕ) for 90 min. After infection, the macrophages were lysed and exposed to heat in order to kill vegetative organisms and preserve spores. Surviving spores were germinated and grown in vitro using rich medium, and then new spores were prepared. These spores were used to infect cultured macrophages, which were again used to enrich for germination-defective mutants. After five rounds of enrichment, individual clones were examined by RATE reaction to determine where the transposon was inserted into the genome of the germination defective mutant. (B) Bar graph representing the percentage of heat-resistant spores represented in the population following the steps of enrichment. Aliquots were collected at each of the first three rounds of enrichment, and the total CFU and heat resistant CFU were determined and used to calculate the percentage of spores in the population.

After three washes with PBS, the cells were permeabilized with 0.1% Triton X-100 in PBS for 5 min and then washed again three times in PBS. Washed cells were then stained for F-actin with 1 U of Alexa Fluor 568-phalloidin (Molecular Probes)/coverslip for 30 min. After three final rinses in PBS, the coverslips were mounted onto glass slides using ProLong Gold antifade reagent with DAPI (4′,6′-diamidino-2-phenylindole; Molecular Probe). Fluorescent confocal laser scanning microscopy was conducted with a Zeiss LSM-510 META laser scanning confocal microscope using the Leica confocal software (LCS Lite).

Quantification of germination efficiency after macrophage infection. A confluent monolayer of RAW 264.7 macrophages at 7.5×10^5 cells/well was infected with *B. anthracis* Sterne parent strain spores, *B. anthracis* Δ*gerHA*, or *B. anthracis* mini-*Himar1* spores at an MOI of 10 for 30 min, followed by treatment with gentamicin (10 μg/ml) for an additional 30 min. Macrophages were subsequently washed 10 times in growth medium and incubated at 37°C for 12 h, at which point the macrophages were harvested and the cell lysate was collected. Half of the sample was serially diluted in PBS and plated on LB agar. The other half was heated to 70°C for 45 min in order to heat kill any spores that germinated, after which serial dilutions were plated. The percentage of spores resistant to heat treatment was then calculated by enumerating the CFU following an overnight incubation. These were divided by the total CFU obtained without heating and multiplied by 100 in order to determine the percent germination for each experimental condition. Three experiments were performed, and the averages and standard deviations were determined.

Spore germination analysis. In vitro spore germination was monitored spectrophotometrically where changes in refractive index (i.e., the optical density at 600 nm) are known to occur during transition from spores to vegetative forms of the organism (12). The germinants used were are as follows: L-alanine at 0.5 mM, inosine at 1 mM, and all other amino acids (L-proline, L-tryptophan, etc.) at 50 mM unless otherwise noted. Endospores and experimental germinants were individually suspended at a 2× concentration in PBS and then mixed in a 1:1 ratio to initiate the germination reaction. Spores (3×10^7) were heat activated at 70°C for 45 min before resuspension in 200 μl of germination buffer (PBS with different germinants) to an A_{600} of 0.5 in the well of a 100-well Honeycomb 2 microplate (Thermo Electron Corp.). Spore germination was evaluated based on the decrease in A_{600} over a 90-min time period in a Bioscreen plate reader (Bioscreen C) with constant shaking at 37°C. Experiments were performed in triplicate with at least two different independent spore preparations, and the mean absorbance was determined. For all medium conditions used, standard deviation calculations were consistently <2% of the average value and therefore were not presented on the graphs.

Statistical analysis. Experiments requiring statistical analysis were performed in triplicate, as indicated and analyzed by using the statistics module of Excel. Significance was determined by using a standard two-tailed Student *t* test with an alpha value of 0.05.

RESULTS

Overview of protocol to identify *B. anthracis* genes necessary for intracellular germination. In order to identify genes that are critical for intracellular germination of *B. anthracis*, we designed an approach that enriched for mutants delayed or defective in germination during infection of cultured macrophages. To accomplish this, spores were prepared from a *B. anthracis Himar1*-based mini-transposon library and used to infect RAW 264.7 macrophagelike cells in culture medium. As outlined in Fig. 1A, macrophages were infected with the *B. anthracis Himar1* spores at an MOI of 10. After a 90-min incubation, the cells were subsequently washed 10 times with culture medium and lysed to release intracellular forms (vegetative or spore) of *B. anthracis Himar1*. To eliminate intracellular germinated forms of *B. anthracis Himar1* (i.e., those lacking the targeted phenotype) and preserve mutants of interest (i.e., those delayed in germination), the lysate was heated at 70°C for 45 min, thereby killing vegetative forms of the organism. Surviving mutants (presumptive germination defective) were then inoculated into liquid medium and grown under routine culture conditions to expand the population of survivors from the treatment protocol. Next, fresh spores were prepared from this culture, and the spores were again subjected to the steps in infection and selection for mutants de-

TABLE 1. MIGD clones identified during enrichment

Gene(s)[a]	Description	Genotype	No. of clones[b] (% of total)	*B. anthracis* strain
BAs2807/BAs2808	Insertion between BAs2807 (449 bp at the 5′ side of major facilitator family transporter) and BAs2808 (298 bp at the 5′ side of glycosyltransferase, group 2 family protein)		41 (36.28)	MIGD101
BAs4630	Spore germination protein GerHA	*gerHA*::Tn*Himar1*	24 (21.24)	MIGD102
BAs4631	Spore germination protein GerHB	*gerHB*::Tn*Himar1*	10 (8.85)	MIGD103
BAs4632	Spore germination protein GerHC	*gerHC*::Tn*Himar1*	2 (1.77)	MIGD104
BAs0229	Major facilitator transporter	BAs0229::Tn*Himar1*	10 (8.85)	MIGD105
BAs5014	Hypothetical protein	BAs5014::Tn*Himar1*	7 (6.19)	MIGD106
BAs5265	cGMP specific and stimulated phosphodiesterase/ adenylate cyclase	BAs5265::Tn*Himar1*	6 (5.31)	MIGD107
BAs0177	ABC transporter, substrate-binding protein, putative	BAs0177::Tn*Himar1*	1	MIGD108
BAs0194	Conserved domain protein	BAs0194::Tn*Himar1*	1	MIGD109
BAs0437	Phage transcriptional regulator, ArpU family	BAs0437::Tn*Himar1*	1	MIGD110
BAs4927	Conserved domain protein	BAs4927::Tn*Himar1*	1	MIGD111
BAs5220	Multidrug resistance protein, putative	BAs5220::Tn*Himar1*	1	MIGD112
GBAA pXO1-0130/GBAA pXO11-0218	Insertion between GBAA pXO1-0130 and GBAA pXO11-0218		3 (2.66)	MIGD113
GBAA pXO1-0122/GBAA pXO1-0123	Insertion between GBAA pXO1-0122 and GBAA pXO1-0123		1	MIGD114
GBAA pXO1-0064	Conjugation protein, TraG/TraD family	pXO10064::Tn*Himar1*	1	MIGD115
GBAA pXO1-0108	Putative membrane protein	pXO10108::Tn*Himar1*	1	MIGD116
GBAA pXO1-0164	*pagA*, protective antigen	pXO10164::Tn*Himar1*	1	MIGD117
GBAA pXO1-0224	Conserved hypothetical protein	pXO10224::Tn*Himar1*	1	MIGD118

[a] BLASTn analysis was performed using the genome of *B. anthracis* Sterne and the NCBI nonredundant GenBank database as necessary. In all cases, only significant hits (e value cutoff of $<10^{-4}$) are listed.
[b] That is, the number of candidate clones for which a nonambiguous sequence was obtained via RATE analysis.

layed in germination. Overall, the selection, culture expansion, spore preparation, and new infection cycle was repeated four times over the course of 3 months for a total of five cycles of enrichment. Several permutations of this protocol were also tested, including reducing the MOI from 10 to 1 and reducing the time of infection from 90 to 60 min. However, these differences in the protocol did not dramatically change the overall efficiency of enrichment for germination-defective mutants.

To confirm that the enrichment protocol selected for mutants defective in germination, comparisons were made between infections with spores from *B. anthracis* Sterne 7702 (parent strain) and spores prepared from the *B. anthracis Himar1* library. Samples were collected during passages through the enrichment protocol and examined for relative increases in the number of ungerminated spores. When spores from the parent strain were subjected to this enrichment, the level of surviving spores in the population did not exceed 0.1% of the total CFU. When the surviving spores were expanded in liquid medium and used to infect macrophages, there was no further increase in the percentage of spores surviving the infection (data not shown) using the parent strain. In contrast, as shown in Fig. 1B, when spores from the *B. anthracis Himar1* library were subjected to this enrichment, there was a steady increase in the percentage of spores surviving infection of cultured macrophages. Assessment after the third round of infection and enrichment found that ca. 80% of the population consisted of spores that did not germinate within the first hour after infection of cultured macrophages. Collectively, these observations indicated that this protocol enriched for mutants delayed in germination within the macrophage.

Genetic mapping and identification of *Himar1*-disrupted genes. After the fifth round of enrichment, individual mutants were examined to determine the location of transposon insertions within the genome of *B. anthracis*. Lysates from the fifth round of infection were collected, and heat-resistant (presumptive spores) fractions were plated for isolated colonies on solid agar. A total of 136 individual colonies were picked from solid agar and grown in LB broth, and chromosomal DNA was isolated from each of these candidates. To determine the genetic site where *Himar1* transposed into the genome of each candidate clone, we used a previously described technique, RATE (14). The products of the RATE reaction were sequenced, and a BLASTn analysis was used to determine the site of insertion. Of the 136 clones examined, 113 provided nonambiguous DNA sequence sufficient to determine the site of *Himar1* insertion within the genome.

Table 1 lists the sites of *Himar1* insertion in clones with intracellular germination defects. In all, 18 different genetic loci were identified in the putative germination-defective mutants. Of the 113 clones examined, 41 were found to have an insertion in an approximately 750-bp intergenic region between BAs2807 and BAs2808, and this mutant was termed MIGD101 (for macrophage intracellular germination defective 101). The high representation of MIGD101 appeared to be the result of a clonal expansion of this mutant during the enrichment, since each MIGD101 mutant contained a transposon insertion at exactly the same location in the intergenic region. Transposon insertion was also found with relatively high frequency in genes encoding germination-related proteins GerHA, GerHB, and GerHC, indicating that the enrichment protocol selected for genes that have previously been shown to control *B. anthracis* germination. Further analysis of mutants represented multiple times were found in genes encoding for a major facilitator transporter protein, hypothetical protein, and

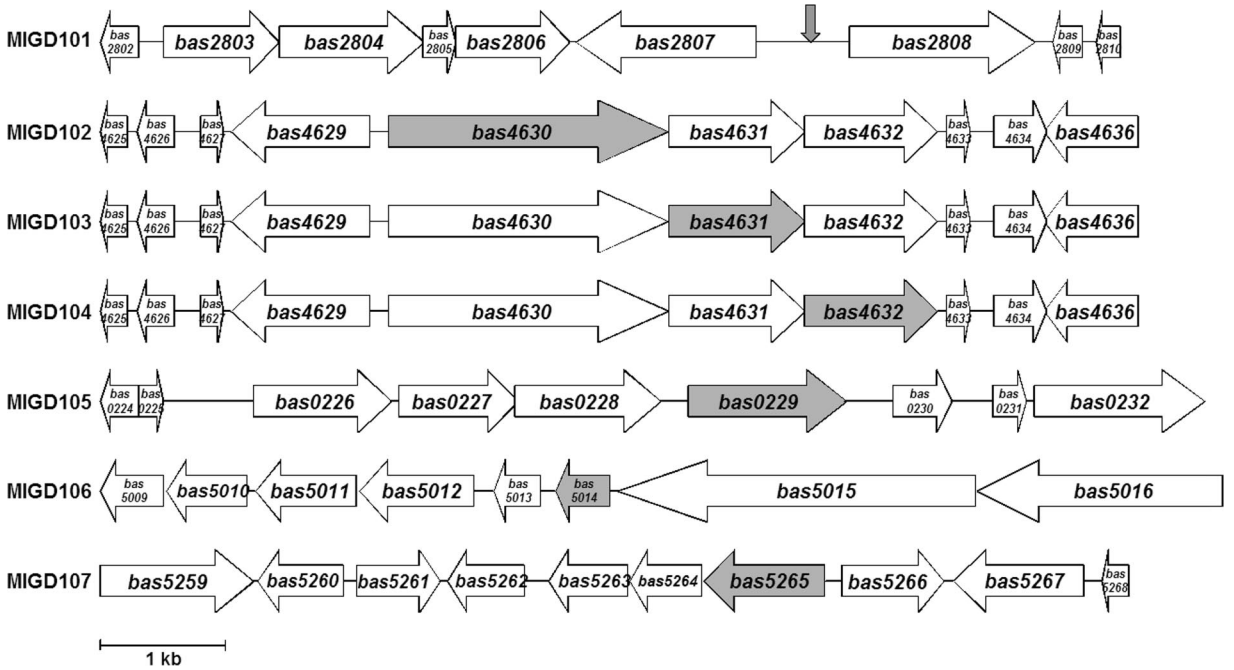

FIG. 2. Genomic location of *Himar1* disrupted genes found multiple times in the population of MIGD mutants. After the enrichment protocol, the location of transposon insertion within the genome of *B. anthracis* 7702 Sterne MIGD mutants was determined by RATE reaction. The disrupted genes are highlighted in gray, and the arrow indicates the site of disruption in an intergenic region.

cGMP-specific and stimulated phosphodiesterase/adenylate cyclase and an intergenic region in the *B. anthracis* Sterne ancestor Ames plasmid, pXO1. The genes represented only a single time were distributed across genes involved in a range of bacterial functions, including conjugation and, interestingly, one hit was detected in *pagA*, the gene encoding protective antigen.

Figure 2 provides a graphic representation of the transposon insertions identified in putative MIGD mutants of *B. anthracis*. As shown in this figure, five of the seven putative MIGD mutants contained transposon insertions in genes found within predicted operon structures. It is unclear whether insertions in operon structures had polar effects, but only the *gerHA*, *gerHB*, and *gerHC* mutants were found in the same operon.

***B. anthracis* MIGD101 is attenuated in macrophage killing.** Experiments next focused on *B. anthracis* MIGD101 in order to further validate the enrichment protocol and better understand the phenotype of this mutant. First, we determined the impact of *B. anthracis* MIGD101 on macrophage survival compared to parent strain *B. anthracis* Sterne and *B. anthracis* Δ*gerHA*, which was first described by Weiner et al. (16, 17) and constructed in a previous study (12).

Extended incubations of *B. anthracis* spores with macrophages eventually leads to the intracellular germination of *B. anthracis* within the macrophages and, subsequently, macrophage cell death (our unpublished observation). This event generally takes up to 12 h and is a simple indicator of the efficiency of infection, germination, growth, and escape of *B. anthracis* during interaction with macrophages. Hence, using a standard spore-macrophage infection assay, macrophages were infected with the spores of parental *B. anthracis* Sterne 7702 strain, *B. anthracis* Δ*gerHA*, and *B. anthracis* MIGD101. After infection for 1 h, macrophages were treated with gentamicin and washed 10 times to reduce levels of extracellular spores or vegetative bacteria. Cell death was then followed by examining changes in LDH levels in the extracellular medium, which is an indicator of changes in plasma membrane integrity corresponding to a loss in cell viability. Samples were collected every hour for 12 h and examined for extracellular levels of LDH. As shown in Fig. 3A, a statistically significant difference in LDH levels was detected between extracellular supernatants of macrophages infected with *B. anthracis* Sterne or the two mutants. Although an increase in LDH release was apparent by 6 h in macrophages infected with spores from the parent strain and *B. anthracis* Δ*gerHA*, LDH release could not be detected at this time point in macrophages infected with *B. anthracis* MIGD101. Overall, macrophages infected with *B. anthracis* parent strain or with *B. anthracis* Δ*gerHA* exhibited almost 100% cell death by 10 h, whereas LDH release was ca. 75% of the total in *B. anthracis* MIGD101 at this time point.

To confirm the LDH observations, we used trypan blue staining to examine the overall profile of viable and nonviable cells in visible fields of infected macrophages. As shown in Fig. 3B to D, at 6 h after infection, >90% of macrophages infected with the parental *B. anthracis* strain stained with trypan blue (which is indicative of cell death) (Fig. 3B), whereas ca. 50% of the macrophages infected with the *B. anthracis* Δ*gerHA* were trypan blue positive (Fig. 3C) and <10% of the *B. anthracis* MIGD101 stained positive for cell death (Fig. 3D). These findings from two independent methods of assessing cell viability demonstrate *Himar1*-mediated disruption of the intergenic region between BAs2807 and BAs2808 attenuates the capacity of *B. anthracis* to kill macrophages after infection in cell culture. The findings from the enrichment protocol and the

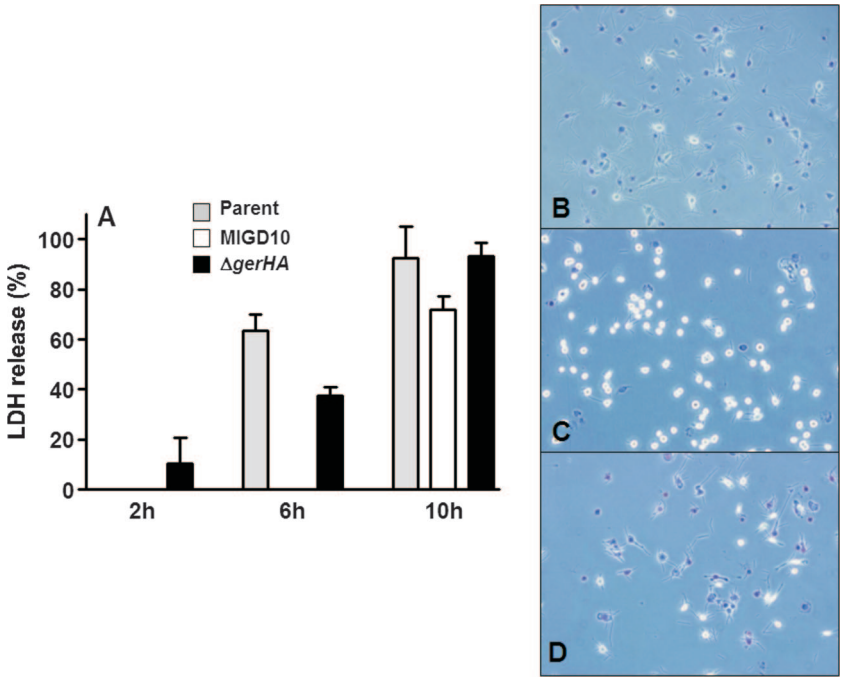

FIG. 3. Macrophage viability after infection with the *B. anthracis* parent strain, the MIGD101 mutant, and the Δ*gerHA* mutant. (A) LDH release in macrophages treated with spores of parent strain, MIGD101, and Δ*gerHA* mutants of *B. anthracis* Sterne 7702. The strains corresponding to each time point and level of LDH release are indicated in the figure. The bar graph indicates the percentage of macrophage LDH released after infection (MOI of 1; $n = 3$). Error bars indicate ± the standard error of the mean. *P* values were determined by comparisons between the parent strain and mutant strains using a two-tailed Student *t* test and found to be <0.05. (B, C, and D) Phase-contrast images of trypan blue-stained cultured macrophages 6 h after infection (MOI of 1) with the *B. anthracis* Sterne 7702 parent strain (B), the *B. anthracis* MIGD101 mutant (C), and the *B. anthracis* Δ*gerHA* mutant (D).

viability assessment support the notion that *B. anthracis* MIGD101 is delayed in germination and attenuated for cell killing during interactions with cultured macrophages.

***B. anthracis* MIGD101 predominantly exists as a spore within infected macrophages.** In order to validate that delays in MIGD101 germination occurred within the intracellular environment of the macrophages, rather than through some undefined extracellular or cell surface interaction, we used differential staining and confocal microscopy to directly visualize spores within infected cells. To accomplish this, spores from the parental *B. anthracis* Sterne 7702 strain, *B. anthracis* Δ*gerHA*, or *B. anthracis* MIGD101 strain were labeled with the fluorescent dye Alexa Fluor 488. Alexa Fluor 488 labeling is specific for the spore coat, and after germination there is a loss in fluorescence as the dye is shed during outgrowth (our unpublished observations). Hence, the loss of the *B. anthracis*-associated dye could be due to germination or clearance of the spores. Thus, to detect vegetative forms of *B. anthracis* that arise after germination, infected macrophages were subjected to an additional step of staining with the DNA-specific dye DAPI. During pilot experiments, we demonstrated that vegetative forms, but not spore forms, of *B. anthracis* were susceptible to DAPI staining, presumably due to the exclusion of the dye by the spore coat. The DAPI staining also provided a visual orientation of the spore location within the cell, because the macrophage DNA was also stained, thereby marking the nucleus. Finally, to provide a visual outline of the cell, macrophages were stained with a third dye, Alexa Fluor 568-phalloidin, which labels actin. Within the confocal microscopy images, spores appear green, vegetative forms appear blue, the nucleus appears blue, and microtubules are red.

Macrophages were infected with Alexa Fluor 488-labeled spores at an MOI of 1 and examined at 1, 6, and 12 h postinfection. Within 1 h, spores were detected in macrophages infected with parent strain *B. anthracis*, *B. anthracis* Δ*gerHA*, and *B. anthracis* MIGD101 (Fig. 4). By 6 h after infection, the levels of detectable spores were markedly reduced in macrophages infected with *B. anthracis* parent strain or *B. anthracis* Δ*gerHA*. In contrast, at the 6-h time point *B. anthracis* MIGD101 spores were at levels similar to the 1-h infection. By 12 h after infection, macrophages were lysed in the *B. anthracis* parent strain infection, a finding indicative of cell death and corresponding to the results of the LDH and trypan blue experiments. Extracellular *B. anthracis* parent strain was detected as vegetative forms by DAPI staining, supporting the idea that the organism had germinated, grown, escaped, and lysed the macrophages. At the 12-h time point, macrophages treated with *B. anthracis* Δ*gerHA* demonstrated a mixed population of lysed and apparently intact cells containing vegetative forms of *B. anthracis* detected by DAPI staining. At the 12-h time point after infection with *B. anthracis* MIGD101, a majority of the population of macrophages contained a mixture of vegetative bacilli and spores. A similar analysis was performed using an MOI of 10 in an effort to obtain a more robust phenotype. As shown in Fig. 4D, H, and L, at this higher MOI a mixture of spores and vegetative bacilli were detected in macrophages infected with

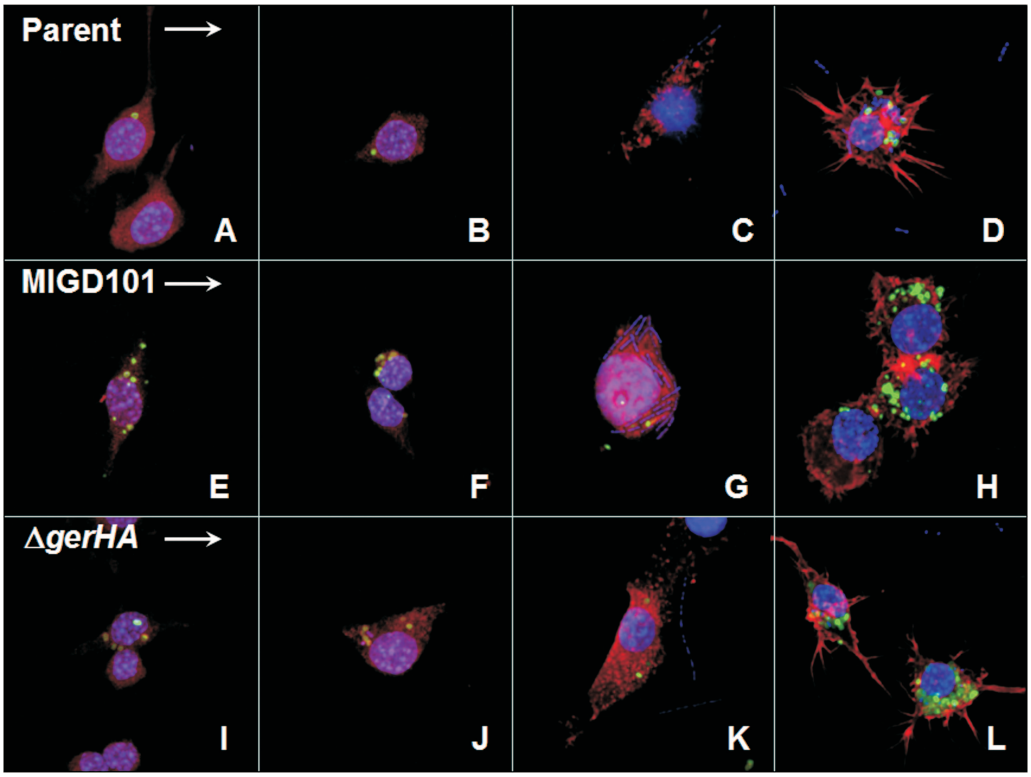

FIG. 4. Detection of spores and vegetative *B. anthracis* in RAW 264.7 macrophages by using confocal microscopy. In order to detect spores within infected macrophages, spores of the parent strain and the mutants were labeled with Alexa Fluor 488 (green). Vegetative *B. anthracis* were visualized by staining DNA with DAPI (blue), which labels DNA from vegetative bacilli and the chromosomal DNA in the macrophage nucleus. Macrophages are highlighted by staining F-actin with Alexa Fluor 568-phalloidin (red). Confocal images display macrophage infections with the *B. anthracis* parent strain (A to D), the *B. anthracis* MIGD101 mutant (panels E to H), and *B. anthracis* Δ*gerHA* mutant (I to L). Infections are shown with an MOI of 1 after 1 h (A, E, and I), 6 h (B, F, and J), and 12 h (C, G, and K). Infections with an MOI of 10 after 1.5 h are shown in panels D, H, and L.

B. anthracis parent strain or with *B. anthracis* Δ*gerHA*; however, in line with the infection at an MOI of 1, *B. anthracis* MIGD101 was only detected as a spore at this stage of infection. These data are consistent with the idea that the observed phenotype of *B. anthracis* MIGD101 is due to a delay in the germination of this mutant inside of cultured macrophages.

Differential heat resistance of *B. anthracis* MIGD101 after macrophage infection reflects delays in germination. One of the hallmarks of the initiation of germination is increased sensitivity of *B. anthracis* to heat, whereas dormant spores are resistant to heat. The results from the enrichment protocol suggested that *B. anthracis* MIGD101 was resistant to heat, suggesting that spores prepared from this mutant remain dormant for an extensive period of time following uptake by macrophages. The qualitative results from confocal microscopy also supported the idea that *B. anthracis* MIGD101 was dormant. To prove this in a quantitative manner for *B. anthracis* MIGD101, we used a previously described macrophage infection protocol (7, 12) that quantified the overall percentage of dormant spores in the population across a time course of infection. To accomplish this, macrophages were infected with parental *B. anthracis* Sterne 7702 strain, *B. anthracis* Δ*gerHA*, or *B. anthracis* MIGD101 and, after the cells were treated with gentamicin and washed 10 times to reduce extracellular bacteria, the cells were lysed. The heat-resistant and heat-sensitive CFU in each of the samples were then calculated as described in Materials and Methods. As shown in Fig. 5, after 12 h of infection with *B. anthracis* <2% of the organisms were detected as spores. In contrast, *B. anthracis* Δ*gerHA* and *B. anthracis* MIGD101 exhibited a high level (37 and 50%, respectively) of spores even after this extended infection. These findings confirm and quantify the observations from the en-

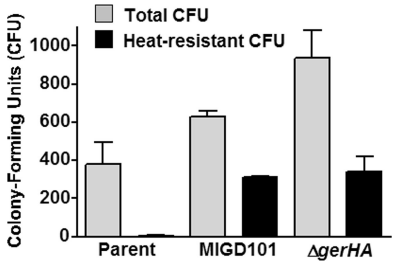

FIG. 5. Quantitative comparison of spore-macrophage interactions between the *B. anthracis* parent strain, the MIGD101 mutant and the Δ*gerHA* mutant. Spores were incubated with RAW 264.7 macrophages at an MOI of 10. After a 12-h incubation, spores and vegetative *B. anthracis* were collected, and CFU were counted prior to and after a 70°C incubation for 45 min. The bar graph presents the total CFU and the heat-resistant CFU ($n = 3$). Error bars indicate ± the standard error of the mean, and the P values were <0.05.

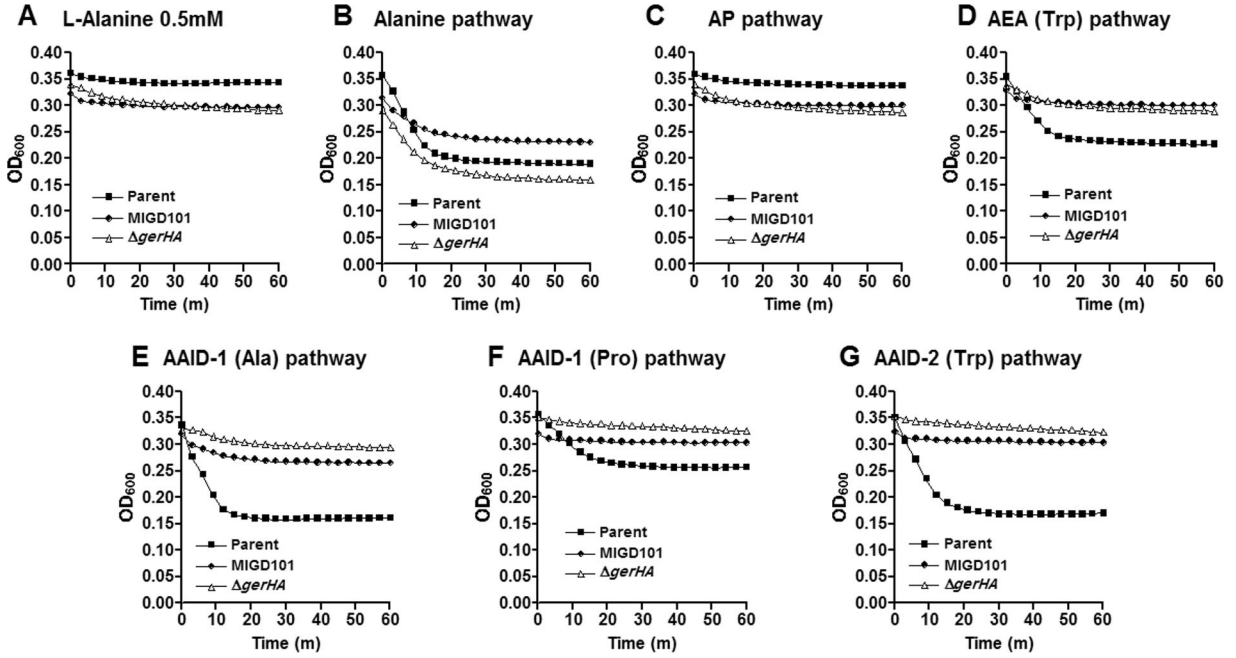

FIG. 6. Analysis of in vitro spore germination pathways utilized by *B. anthracis*. Spores of parent strain *B. anthracis*, *B. anthracis* MIGD101, and *B. anthracis* Δ*gerHA* were treated with germinants and cogerminants that stimulate each of the known germination pathways. Spores were incubated in PBS with different germinants at the following concentrations: L-alanine, 0.5 mM; inosine, 1 mM; and all other amino acids (L-proline, L-tryptophan, etc.), 50 mM unless otherwise noted. Germination was monitored spectrophotometrically by changes of refractive index at an optical density at 600 nm for 60 min. The results are the average of three experiments and, for all pathways, the standard deviation did not exceed 2% from the average value and therefore is not presented in the graphs. (A) L-Alanine (0.5 mM); (B) alanine (Ala) pathway (50 mM L-alanine); (C) alanine-proline (AP) pathway (0.5 mM L-alanine, 50 mM L-proline); (D) aromatic amino acid-enhanced alanine (AEA) pathway (0.5 mM L-alanine, 50 mM L-tryptophan); (E) amino acid and inosine dependent pathway (AAID-1) (1 mM concentration of inosine pairs, 0.5 mM L-alanine); (F) 50 mM L-proline pathway (50 mM L-proline); (G) AAID-2 pathway (1 mM inosine, 50 mM L-tryptophan).

richment protocol and confocal analysis, which suggested that *B. anthracis* MIGD101 is delayed in intracellular germination.

In vitro germination defects of MIGD101. Previous studies by Fisher and Hanna demonstrated that *B. anthracis* is subject to regulation by five distinct germination pathways (6). These pathways are defined by their sensitivity to different germinants and cogerminants, consisting of combinations of alanine, aromatic amino acids, and purine ribonucleosides. The alanine-proline, aromatic amino acid-enhanced alanine, amino acid and inosine-dependent 1 and 2, and the concentration L-alanine pathways were tested for the activation of MIGD101 germination. Freshly prepared spores from the parental *B. anthracis* Sterne 7702 strain, *B. anthracis* Δ*gerHA*, and *B. anthracis* MIGD101 were incubated under conditions that activated each of the germination pathways. As shown in Fig. 6, similar to the parent strain and *B. anthracis* Δ*gerHA*, *B. anthracis* MIGD101 germinated in the presence of 50 mM L-alanine. However, in contrast to the parent strain but similar to *B. anthracis* Δ*gerHA*, *B. anthracis* MIGD101 was defective in all other germination pathways.

DISCUSSION

Results from the recent studies reveal a panel of bacterial genes involved in the intracellular germination of *B. anthracis.* The data obtained in the present study further support the idea that the intracellular germination of *B. anthracis* is both multifactorial and complex. Eighteen different genetic loci were identified as putative contributors to intracellular germination of *B. anthracis*. Genes previously associated with intracellular germination were found in the enriched pool of mutants, supporting the idea that the protocol was effective at identifying mutants attenuated for germination. Moreover, we were able to demonstrate that enrichment for germination-defective mutants required transposon mutagenesis, suggesting that the frequency of random mutations that give rise to the phenotype of interest is low.

There are several interesting correlates between the panel of candidate genes and the observed phenotype. First, many of the MIGD-related genes encode for membrane-associated proteins, and it will be of interest in future studies to specifically determine whether these proteins function in both their predicted roles and germination. Second, the frequency of MIGD mutants with transposon insertions in pXO1 is striking. Eight of the 18 mutants contained insertions in pXO1. We recognize the possibility that the high frequency of insertions in pXO1 may be due to preferential insertion of the *Himar1* transposon into this plasmid. However, it is worth noting that the presence of pXO1 is one of the distinguishing factors between pathogenic *B. anthracis* and nonpathogenic *Bacillus* species. Historically, the virulence of *B. anthracis* has been attributed to the presence of pXO1 because this plasmid encodes for the genes of anthrax toxin. In light of the current findings, it now is also reasonable to suggest that pXO1 could support effective intracellular germination of *B. anthracis*,

which would contribute to the virulence of this pathogen. Indeed, Guidi-Rontani et al. have previously reported that genes of the *gerX* operon on pXO1 are critical to the germination of *B. anthracis* spores (8). It should be noted that mutants in the *gerX* operon were not identified in our enrichment, and this may reflect the fact that some germination mutants are likely to exhibit such a strong defect in germination that they cannot be enriched during the step of expanding the mutants in vitro under nutrient-rich conditions. Third, the identification of an MIGD mutant with an insertion in *pagA* further supports the reported observations of Guidi-Rontani et al. found that protective antigen (the protein encoded by *pagA*) is involved in the intracellular activities of *B. anthracis* (7, 9).

The findings from the present study also correlate with transcriptional profiling data obtained by Bergman et al., which identified genes differentially expressed by *B. anthracis* after infection of phagocytic cells (1). Strikingly, 5 of the 18 genes identified in the current study were also found in the earlier study to be differentially expressed by *B. anthracis* after infection of phagocytic cells. Collectively, BAs0177 (94% identity with GBAA0175), BAs0437 (100% identity with GBAA0457), GBAA_pXO1_0164 (*pagA*), GBAA_pXO1_0064, and GBAA_pXO1_0108 were shown to be differentially expressed by *B. anthracis*. These genes were also found to be essential for intracellular germination as well, suggesting the proteins expressed from these genes could contribute to both germination and the growth of *B. anthracis* within an intracellular environment.

The data shown in Fig. 3 to 6 support the idea that MIGD101 is defective in intracellular germination and macrophage killing and is unable to germinate in the presence of several well-established germinants. Indeed, MIGD101 exhibits a phenotype similar to a *gerHA* mutant; however, analysis of the *gerHA* operon in this mutant confirmed that there was not a second site mutation or transposon insertion in the *gerH* genes (data not shown). The site of transposon insertion does not appear to interrupt the promoter regions of BAs2807 or BAs2808 and, based on preliminary experiments, both of these genes appear to be transcribed similar to the wild type (data not shown). As with most bacteria, the role of intergenic regions in the physiology of *B. anthracis* remains poorly understood. Continued studies on the MIGD101 mutant will help elucidate how this intergenic region contributes to the intracellular germination and physiology of *B. anthracis*.

In a recent study, Day et al. used transposon site hybridization analysis to identify genes necessary for germination, growth, and sporulation of *B. anthracis* in culture medium (3). Several genes encoding for germination and sporulation factors were identified by using the transposon site hybridization approach but, in contrast, data from our experiments indicate that *B. anthracis* may use a much more extensive repertoire of proteins to germinate after encountering the intracellular environment of mammalian cells. Fewer than a third of the candidate genes identified in the present study have been associated with germination, indicating that *B. anthracis* intracellular germination may be a more complex process than that observed under defined extracellular conditions.

The transient survival and germination of *B. anthracis* in intracellular environments is thought be an important step in the progression of anthrax disease. Overall, the results presented here provide insight into the complexity of *B. anthracis* genes that are involved in this process.

Editor: J. L. Flynn

ACKNOWLEDGMENTS

This study was supported by a Public Health Service grant U54AI057156, the Western Region Center for Biodefense and Emerging Infectious Diseases (J.D.B., S.R.B., and T.M.K.), and Public Health Service grant AI33537 to T.M.K.

REFERENCES

1. **Bergman, N. H., E. C. Anderson, E. E. Swenson, B. K. Janes, N. Fisher, M. M. Niemeyer, A. D. Miyoshi, and P. C. Hanna.** 2007. Transcriptional profiling of *Bacillus anthracis* during infection of host macrophages. Infect. Immun. **75:**3434–3444.
2. **Cataldi, A., E. Labruyere, and M. Mock.** 1990. Construction and characterization of a protective antigen-deficient *Bacillus anthracis* strain. Mol. Microbiol. **4:**1111–1117.
3. **Day, W. A., Jr., S. L. Rasmussen, B. M. Carpenter, S. N. Peterson, and A. M. Friedlander.** 2007. Microarray analysis of transposon insertion mutations in *Bacillus anthracis*: global identification of genes required for sporulation and germination. J. Bacteriol. **189:**3296–3301.
4. **Dixon, T. C., A. A. Fadl, T. M. Koehler, J. A. Swanson, and P. C. Hanna.** 2000. Early *Bacillus anthracis*-macrophage interactions: intracellular survival and escape. Cell Microbiol. **2:**453–463.
5. **Dixon, T. C., M. Meselson, J. Guillemin, and P. C. Hanna.** 1999. Anthrax. N. Engl. J. Med. **341:**815–826.
6. **Fisher, N., and P. Hanna.** 2005. Characterization of *Bacillus anthracis* germinant receptors in vitro. J. Bacteriol. **187:**8055–8062.
7. **Guidi-Rontani, C., M. Levy, H. Ohayon, and M. Mock.** 2001. Fate of germinated *Bacillus anthracis* spores in primary murine macrophages. Mol. Microbiol. **42:**931–938.
8. **Guidi-Rontani, C., Y. Pereira, S. Ruffie, J. C. Sirard, M. Weber-Levy, and M. Mock.** 1999. Identification and characterization of a germination operon on the virulence plasmid pXO1 of *Bacillus anthracis*. Mol. Microbiol. **33:**407–414.
9. **Guidi-Rontani, C., M. Weber-Levy, E. Labruyere, and M. Mock.** 1999. Germination of *Bacillus anthracis* spores within alveolar macrophages. Mol. Microbiol. **31:**9–17.
10. **Hu, H., J. Emerson, and A. I. Aronson.** 2007. Factors involved in the germination and inactivation of *Bacillus anthracis* spores in murine primary macrophages. FEMS Microbiol. Lett. **272:**245–250.
11. **Ireland, J. A., and P. C. Hanna.** 2002. Macrophage-enhanced germination of *Bacillus anthracis* endospores requires *gerS*. Infect. Immun. **70:**5870–5872.
12. **McKevitt, M. T., K. M. Bryant, S. M. Shakir, J. L. Larabee, S. R. Blanke, J. Lovchik, C. R. Lyons, and J. D. Ballard.** 2007. Effects of endogenous D-alanine synthesis and autoinhibition of *Bacillus anthracis* germination on in vitro and in vivo infections. Infect. Immun. **75:**5726–5734.
13. **Oliva, C. R., M. K. Swiecki, C. E. Griguer, M. W. Lisanby, D. C. Bullard, C. L. Turnbough, Jr., and J. F. Kearney.** 2008. The integrin Mac-1 (CR3) mediates internalization and directs *Bacillus anthracis* spores into professional phagocytes. Proc. Natl. Acad. Sci. USA **105:**1261–1266.
14. **Ribot, E. M., F. D. Quinn, X. Bai, and J. J. Murtagh, Jr.** 1998. Rapid amplification of transposon ends for the isolation, cloning and sequencing of transposon-disrupted chromosomal genes. BioTechniques **24:**16–17, 20, 22.
15. **Sanz, P., L. D. Teel, F. Alem, H. M. Carvalho, S. C. Darnell, and A. D. O'Brien.** 2008. Detection of *Bacillus anthracis* spore germination in vivo by bioluminescence imaging. Infect. Immun. **76:**1036–1047.
16. **Weiner, M. A., and P. C. Hanna.** 2003. Macrophage-mediated germination of *Bacillus anthracis* endospores requires the *gerH* operon. Infect. Immun. **71:**3954–3959.
17. **Weiner, M. A., T. D. Read, and P. C. Hanna.** 2003. Identification and characterization of the *gerH* operon of *Bacillus anthracis* endospores: a differential role for purine nucleosides in germination. J. Bacteriol. **185:**1462–1464.